JOURNAL OF APPLIED ELECTROCHEMISTRY 19 (1989) 789–801

REVIEW PAPER

Electrochemical properties of metal–molten salt mixtures

G. M. HAARBERG, J. THONSTAD

Laboratories of Industrial Electrochemistry, University of Trondheim, The Norwegian Institute of Technology, 7034 Trondheim, Norway

Received 22 September 1988; revised 12 January 1989

Available literature on metal–molten salt mixtures is reviewed with emphasis on electrochemical properties of the dissolved metal in dilute solutions of metals in salts. Phase diagrams and solubility data are summarized, followed by a more detailed treatment of conductivities, migration studies, emf, anodic oxidation, measurements of electronic conduction, etc. Some structural models are discussed.

1. Introduction

1.1. *Industrial background*

Molten salts have a wide industrial application, and industrial production of metals by molten salt electrolysis has become a large industry. Important processes are production of aluminium from a fluoride–alumina melt at ~960° C, magnesium from a chloride melt at ~700° C and sodium from a chloride melt at ~750° C. Smaller quantities of lithium, potassium, rubidium, calcium, beryllium, zirconium, tantalum and titanium are also produced by molten salt electrolysis either directly or indirectly by metallothermic reaction using aluminium, magnesium or sodium as reducing agents. Related processes are metal refining (Al, Ti) and electroplating of metals. Electroplating of refractory metals from molten salts is a new and promising field.

In electrolytic processes it is important to operate at a minimum consumption of energy and at the highest possible current efficiency. Loss of metal during electrolysis is primarily due to the reoxidation between the metal and the anode product by dissolution of metal in the electrolyte. Electroactive impurities in the electrolyte may also affect the current efficiency as well as evaporation of metal and reaction with the cell lining. Loss in current efficiency related to dissolved metal is caused by: dissolution of metal in the electrolyte; mass transfer of dissolved metal towards the anode; ionic migration of dissolved metal; electronic conductivity of dissolved metal; back reaction between dissolved metal and the anode product; anodic oxidation of dissolved metal; evaporation of metal-containing species.

The major part of the loss in current efficiency in industrial processes is due to dissolved metal. Since the dissolved metal plays such an important role during molten salt electrolysis, it is of interest to clarify its properties. With proper knowledge of metal solubility, mass transfer and electronic conductivity the current efficiency can in principle be predicted. In the absence of convective mixing, diffusion, migration and electronic conductivity set the limit for the maximum attainable current efficiency.

There are certain ways to reduce the negative influence of dissolved metal which one takes advantage of in the electrolytic process: (i) the use of mixtures of molten salts leads to decreased metal solubility; this is also attained by lower temperature, however, addition of salts may lead to codeposition of other metals; (ii) good separation of the anode and cathode compartments reduces the rate of the back reaction.

Typical data for metal solubilities and for current efficiency and energy consumption in the industrial processes for production of aluminium, magnesium and sodium are given in Table 1. The solubilities are low except in the case of sodium where a diaphragm is used for separation.

1.2. *Mixtures of metals and molten salts. General description*

The mixtures of metals and molten salts discussed in the present treatment will mainly be restricted to systems where the metal dissolves in a pure molten halide with the corresponding metal cation. Since around 1960 this field has received much attention, and there exist a great number of data, such as phase diagrams and electrical conductivities, which make it possible to compare the various systems. Several authors have tried to classify the different mixtures of metals and molten salts into categories which reflect their properties.

The first observations made of interactions between molten salts and metals arose from simple electrolysis experiments. So-called metal fog and metal streamers coming from the cathode, coloured melts and low current efficiency are key words. It was once assumed that the metal was dispersed in the melt with the formation of so-called 'pyrosols'. Early in this century systematic examination of the properties of some mixtures of metals and molten salts started. Aten [5, 6]

Table 1. Molten salt electrolysis. Metal solubility in the electrolyte and typical ranges of current efficiency (CE) and energy consumption (W_{el}) *in industrial production of Al, Mg, Na*

Metal	*Electrolyte*	*Temperature (°C)*	*Metal solubility (wt %)*	*CE*	W_{el} *(kWh kg^{-1})*	*References*
Al	AlF_3–NaF–Al_2O_3	950–980	$\simeq 0.1$	0.88–0.94	13–16	[1]
Mg	NaCl–KCl–$CaCl_2$–$MgCl_2$	700–750	$\simeq 0.01$	0.80–0.90	13–18	[2]
Na	$CaCl_2$–NaCl	600	$\simeq 3.3$	$\simeq 0.80$	10–12	[3, 4]
	$CaCl_2$–$BaCl_2$–NaCl	600	–	0.80–0.90	$\simeq 10$	[3, 4]

determined the phase diagrams and electrical conductivities for the systems $BiCl_3$–Bi and $CdCl_2$–Cd, and Lorenz *et al.* [7] measured the solubility of lead in $PbCl_2$–KCl mixtures. A more comprehensive investigation was later made by Bredig and coworkers [8, 9] by examining physicochemical and electrical properties of mixtures of alkali metals and alkaline earth metals in alkali halides and alkaline earth halides respectively. More advanced experimental techniques have been applied recently, and physicochemical, electrical, electronic, magnetic and electrochemical properties have been determined for a large number of systems. Reviews in this field have been published by Cubicciotti [10], Ukshe and Bukun [11], Bredig [9], Corbett [12] and Warren [13, 14].

In most cases the properties of the pure molten salt will change when a metal dissolves in it, and a true solution is formed. Under certain conditions however, such as during electrolysis, colloidal metal particles may also be formed. Bredig [9] distinguished between two categories of metal-molten salt mixtures: metallic and non-metallic solutions. In metallic solutions the metal dissolves without interacting with the melt. Metal ions and partially free electrons are formed. The presence of free electrons gives rise to electronic conductivity. The total conductivity increases by addition of metal. In non-metallic solutions the metal reacts with the melt under formation of subvalent metal ions or subvalent compounds. The electrical conductivity is affected only to a small extent by addition of metal. Reversible redox couples such as M^{2+}/M_2^{2+} are formed. The dissolved metal can be anodically oxidized and it can migrate in an electric field.

For both metallic and non-metallic solutions the metal will be recovered by cooling a mixture of dissolved metal and molten salt. The distinction between the two models is not sharp. Some systems can be ascribed to both categories depending on the concentration of dissolved metal. When changing other parameters like temperature and pressure the properties of the system may change.

The following typical properties have been observed for mixtures of the metals and molten salts: the solubility is highest for metals in their 'own' salts; the metal solubility increases with increasing temperature; several binary systems show complete miscibility between metal and salt above a certain critical temperature; metal-molten salt systems usually show a continuous transformation from metal to non-metal behaviour when the temperature is sufficiently high.

Bredig's models are still being used to discuss experimental data obtained for mixtures of metals and molten salts. Recent data have contributed to greater understanding in this field, and several theoretical models have been proposed. In particular, interest has been focused on electronic properties.

2. Properties of metal–molten salt mixtures

The present treatment is focused on electrochemical and related properties of dissolved metal in molten salts. Phase diagrams are included as a source of background information. The data considered to be the most reliable have been selected whenever possible. Data concerning other properties are well covered in review papers by Bredig [9] and Corbett [12] and more recently by Warren [13, 14].

2.1. *Visual observations*

Pure molten salts are usually clear and transparent. When a metal dissolves in a pure molten salt a colour change is often observed. The intensity of the colour often increases with increasing concentration of dissolved metal. Solidified melts with dissolved metal are usually grey due to finely dispersed metal. Corbett and coworkers [15–17] studied several systems and noticed colour changes after addition of metal to the pure molten salt. Transport of subhalides from the melt into the gas phase was also examined. Visual observations made during electrolysis are treated in Section 2.4.1.

2.2. *Phase diagrams. Metal solubility*

A great number of phase diagrams have been determined for binary salt–metal systems. In some systems there is total miscibility between metal and salt, in others the metal solubility is very limited at temperatures available at normal pressure. Binary phase diagrams for metal and the corresponding metal halide have been compiled and discussed by Bredig [9]. Some recent studies are quoted in 'Phase Diagrams for Ceramists' [18].

All the phase diagrams are characterized by a lowering of the melting point of the salt by addition of metal. This phenomenon is indicative of true solutions. Several systems exhibit a region with two immiscible liquid phases, i.e. 'a miscibility gap'. Systems with miscibility gaps show positive deviation from Raoult's

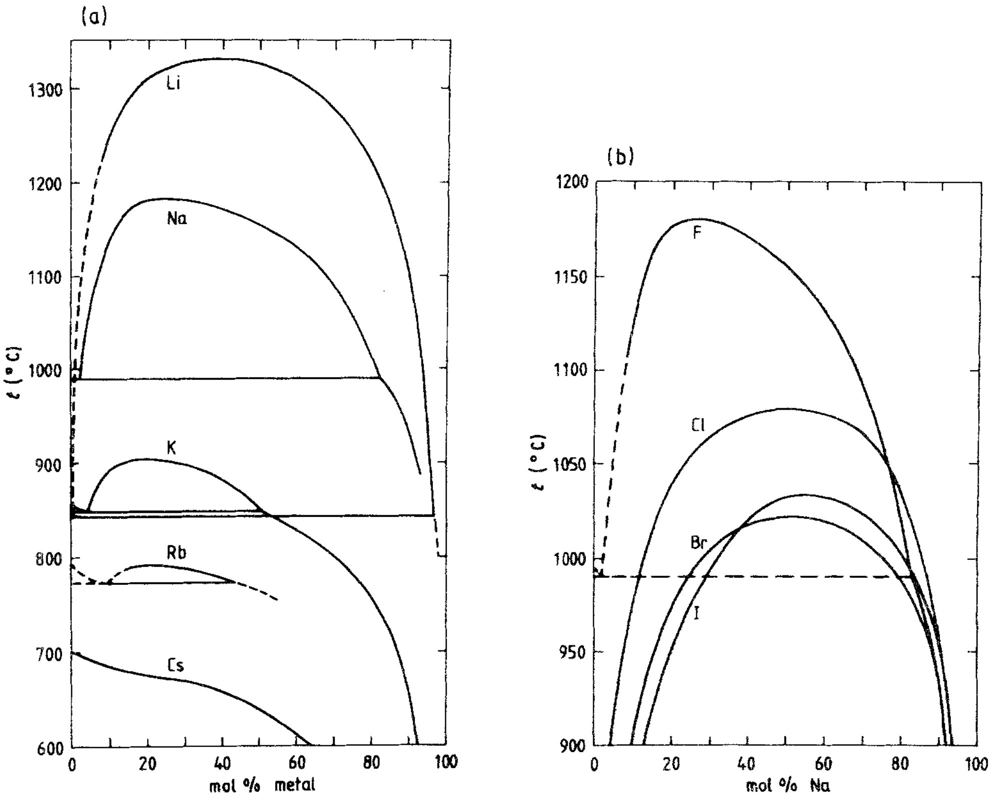

Fig. 1. Phase diagrams for (a) alkali metal–alkali fluorides [19] and (b) sodium–sodium halides [20].

law, i.e. the activity coefficient of the salt is larger than unity. Above a certain temperature, which is called 'the critical temperature of miscibility' or 'the consolute temperature', salt and metal are completely miscible at all compositions. This temperature and the corresponding composition are often selected when making comparisons of various systems.

Some phase diagrams for alkali metal–alkali halide systems are shown in Fig. 1. No solid subhalides exist in these systems. Thermodynamic considerations based on the phase diagrams have led to many speculations and proposals with respect to the structure of these melts, particularly in the salt-rich region. According to Pitzer [21] a mixture of an alkali metal and an alkali halide is formed by mixing the two negative species, halide ions and localized electrons, with the irregular cation lattice. This theory predicts the excess entropy of mixing to be positive. The electrons originate from the valence electrons of the metal and they are localized on anion sites in the lattice, analogous to F-centres in solid crystals. This theory is based on low concentration of dissolved metal.

The phase diagrams for alkaline earth metals–alkaline earth halides are quite similar to those of the alkali systems, but in some cases solid solubility of metal in salt have been reported. The metal solubility in chlorides is found to increase with increasing size of the cation. The calcium systems exhibit miscibility gaps except for the fluoride. No subhalides exist in the solid state. Cryoscopy indicates the presence of subvalent species such as Ca_2^{2+} or Ca^+ in $CaCl_2$–Ca and Mg_2^{2+} or Mg^+ in $MgCl_2$–Mg in the molten mixtures [9].

Phase diagrams and solubility data have been published for several mixtures of rare earth metals and the corresponding halides. These systems show great variation in behaviour. In some of the systems solid subhalides are stable. Many of the other binary mixtures differ from the above-mentioned alkali and alkaline earth systems with respect to phase diagrams and metal solubilities. Solid subhalides exist in some of these systems, and the metal often reacts with the salt forming subvalent ions. The metal solubility is dependent on the tendency to form subhalides. For post-transition metal halides this tendency usually increases with increasing size of the metal ion in each group for a given halide ion. The solubility of a given metal also increases with increasing size of the halide ion except in the Cd and Hg systems. Systems consisting of less electropositive metals are also characterized by very high critical temperatures for miscibility. In particular the bismuth and cadmium systems have been studied.

The phase diagrams for the bismuth–bismuth halide systems which were determined by Yosim *et al.* [22, 23] are shown in Fig. 2. The solubility of Bi above the melting points of the halides is quite high in all three systems. The miscibility gap is reduced and the critical temperature decreases with increasing size of the halide ion. The three systems have in common a subvalent compound 'BiX' which is stable in the solid state. Corbett and coworkers [24, 25] prepared the chloride version of this compound, and by a structural investigation the stoichiometry was found to be $Bi_{12}Cl_{14}(BiCl_{1.167})$. The compound may be expressed by: $(Bi_9^{5+})_2(BiCl_5^{2-})_4(Bi_2Cl_8^{2-})$.

Phase diagrams for the corresponding cadmium

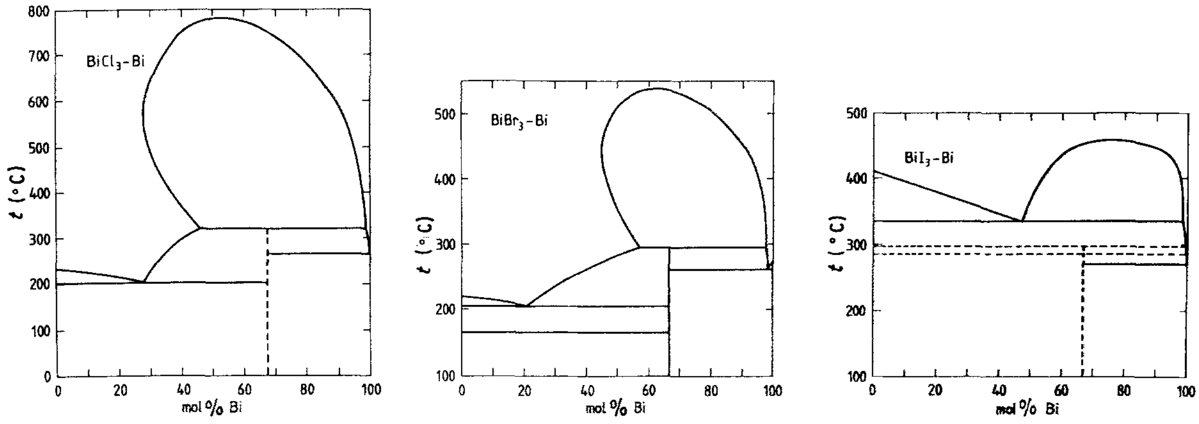

Fig. 2. Phase diagrams for bismuth-bismuth halides [22, 23].

systems were determined by Topol and Landis [26]. There is appreciable solubility of Cd (10–15 mol %) near the melting points of the pure salts. From cryoscopic studies in $CdCl_2$–Cd Grjotheim *et al.* [27] suggested formation of Cd_2^{2+} ions. Cubicciotti [28] determined the solubility of Cd in mixtures of $CdCl_2$ and other chlorides. The solubility of Cd was lowered in all cases ($CeCl_3$, $CaCl_2$, $MgCl_2$, $MnCl_2$, $ZnCl_2$). The decrease in solubility was more pronounced as the added salt contained a more electropositive metal ion or a greater anion to cation ratio. Corbett *et al.* [17] studied the effect on the solubility of Cd by adding $AlCl_3$ to $CdCl_2$. The phase diagram $Cd_2(AlCl_4)_2$–Cd, where the incongruently melting compound $Cd_2(AlCl_4)_2$ appears, was determined. The solubility of Cd was found to be higher in $AlCl_3$-containing melts than in pure $CdCl_2$. The $AlCl_4^-$ ion stabilizes subvalent Cd by complexing with Cd_2^{2+} (or Cd^+).

In $AlBr_3$ and AlI_3 the solubility of Al is very low according to the phase diagrams determined by Thonstad [29]. Studies on the solubility of Al in molten salts have mostly been concentrated on the system NaF–AlF_3–Al_2O_3 [30–34]. In addition to dissolved aluminium also sodium has to be considered, and the solubility is dependent on the composition of the melt, as shown in Table 2. Although there are some differences in numerical values, most authors agree that the solubility decreases with decreasing NaF/AlF_3 ratio and increasing alumina content.

Ødegård *et al.* [32] carried out an extensive study of the effect of several additives on the total solubility, which was summarized by the equation

$$\begin{aligned}\log(c_{Al}) = {} & -1.825 - 0.5919/CR + 3.429 \times 10^3/T \\ & - 3.39 \times 10^{-2}(c_{Al_2O_3}/c_{Al_2O_3(sat)}) \\ & - 2.41 \times 10^{-2} c_{MgF_2} - 2.03 \times 10^{-2} c_{CaF_2} \\ & - 2.49 \times 10^{-2} c_{LiF} \qquad (1)\end{aligned}$$

where CR is the molar NaF/AlF_3 ratio and all concentrations are in wt %, T is the temperature (K), and $c_{Al_2O_3(sat)}$ is the saturation concentration of alumina. Some numerical results for the NaF–AlF_3–Al_2O_3 system based on this equation are given in Table 2. Reaction models were fitted to the experimental data using available activity data and the Temkin model. Near the cryolite composition the two most probable dissolution reactions were

$$Al_{(l)} + 3NaF_{(l)} = AlF_{3(diss)} + 3Na_{(diss)} \qquad (2)$$

$$2Al_{(l)} + AlF_{3(diss)} + 3NaF = 3AlF_2^- + 3Na^+ \qquad (3)$$

Table 2. Solubility of Al in NaF–AlF_3–Al_2O_3 melts

Molar ratio NaF/AlF_3	*T (°C)*	*Al_2O_3 (wt %)*	*Solubility*			*References*
			Al (wt %)	*Na (wt %)*	*Total as Al (wt %)*	
1.7	1000	sat.			0.075	[30]
3.0	1000	sat.	0.065	0.090	0.10	
3.0	1060	sat.			0.14	
6.7	1000	sat.			0.33	
3.0	980	2	0.06	0.12	0.11	[32]
3.0	980	4	0.05	0.09	0.09	
3.0	980	6	0.04	0.08	0.07	
3.0	980	8	0.03	0.06	0.05	
2.25	962	sat.			0.054	[33]
2.25	1000	0			0.076	
3	1000	sat.			0.083	
4	1000	sat.			0.090	

The presence of monovalent aluminium in the form of AlF_2^- rather than Al^+ or AlF has also been suggested by other authors [33, 34] to explain the concentration dependence of the solubility.

Storozhenko [35] and Kudyakov and Smirnov [36] studied the solubility of Al in $AlCl_3$ and mixtures of $AlCl_3$ with NaCl-KCl. The following reaction was suggested for the dissolution of Al

$$2Al + AlCl_3 = 3AlCl \qquad (4)$$

The solubility of Al increased with increasing concentration of $AlCl_3$ in $AlCl_3$-NaCl mixtures, and it reached a minimum in the equimolar mixture which corresponds to the compound $NaAlCl_4$. In pure $AlCl_3$ the solubility of Al was low and it decreased with increasing temperature. In NaCl-KCl-$AlCl_3$ the solubility increased with increasing NaCl/KCl ratio.

2.3. *Electrical conductivity*

Conductivity data give information about the degree of dissociation of the salt into ions and possible formation of complexes or 'free' electrons. Specific conductivity data for metal-molten salt mixtures have been used to demonstrate electronic conductivity due to dissolved metal. In some cases a continuous transition from ionic to metallic conduction has been detected. Theoretical models have been proposed in order to explain the behaviour of the dissolved metal, and these models are often tested against conductivity data.

Experimental conductivity data are presented in different ways.

(1) The measured specific conductivity of the mixture is treated as the sum of the specific conductivity of the molten salt and that of the dissolved metal

$$\kappa_{MX\text{-}M} = \kappa_{MX} + \kappa_M \qquad (5)$$

(2) The electrical conductivity is expressed in terms of equivalent conductivities

$$\Lambda_{MX\text{-}M} = x_{MX}\Lambda_{MX} + x_M\Lambda_M \qquad (6)$$

where x_{MX} and x_M are equivalent fractions of molten salt and dissolved metal, respectively. The equivalent conductivity of the dissolved metal is then

$$\Lambda_M = \frac{\Lambda_{MX\text{-}M} - (1 - x_M)\Lambda_{MX}}{x_M} \qquad (7)$$

(3) An alternative expression is

$$\kappa_{MX\text{-}M} V_{MX\text{-}M} = x_M\Lambda_M + (1 - x_M)\kappa_{MX} V_{MX} \qquad (8)$$

where V stands for molar volumes.

Electrical conductivities have been determined for most of the binary alkali systems in the salt-rich region by Bredig and coworkers [9]. The specific conductivity of the mixtures was found to increase dramatically by addition of metal in all these systems, the increase being larger in the potassium systems than in the corresponding sodium systems. Some results are shown in Fig. 3.

The equivalent conductivity of dissolved metal, Λ_K, calculated from Equation 5 increases strongly with increasing potassium concentration, while Λ_{Na} decreases with increasing Na concentration. Bronstein and Bredig [37] interpreted these results by assuming that the number of free electrons is less in the sodium systems due to formation of dimers like Na_2 and K_2 of which Na_2 is the more stable. In the salt-rich regions the specific conductivity of the mixtures increases with increasing temperature. Above a certain concentration of dissolved metal the temperature coefficient becomes negative as it is for metals. The equivalent conductivity of dissolved metal is likely to increase with increasing metal content also in the sodium systems at higher temperatures. This behaviour was confirmed for NaI-Na at 900° C for more than 10 mol % Na as reported by Bronstein and Bredig [38].

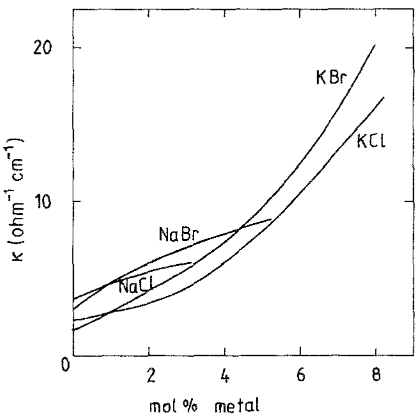

Fig. 3. Specific conductivity of mixtures of sodium-sodium halides and potassium-potassium halides [37]. KCl: 820° C, KBr: 760° C, NaCl: 850° C, NaBr: 805° C.

The equivalent conductivity of dissolved metal at infinite dilution of metal in salt, Λ_M^∞, which is obtained by extrapolating $\Lambda_M - x_M$ plots, has been used to compare the various systems. In the potassium and sodium systems Λ_M^∞ increases with increasing size of the halide ion, and it is higher in the sodium systems. The polarizability of the halide ions increases with size, and high polarizability may facilitate the electron transport.

Warren *et al.* [39] demonstrated that the electron mobility is constant in the NaBr-Na systems at concentrations below 5.5 mol % Na. The observed decrease in equivalent conductivity of dissolved Na in this system was attributed to formation of non-magnetic and non-conducting species which diminish the number of free electrons. Freyland and Nattland [40] studied the temperature dependence on the conductivity in KCl-K mixtures. The activation energy was found to attain a maximum value at a composition which corresponds to the metal-non-metal transition. Formation of localized F-centre electrons at low concentration of dissolved metal was assumed to account for the observed data. Association to F-centre dimers and trimers was likely to occur at higher metal contents. The transition to metallic conduction was observed at a concentration of dissolved potassium approximately half the critical concentration.

Conductivity measurements in alkaline earth metal-

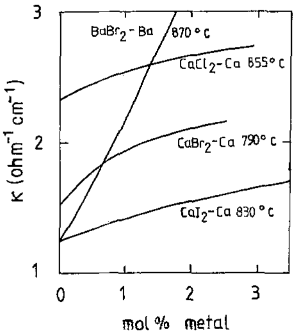

Fig. 4. Specific conductivity of mixtures of alkaline earth metal–alkaline earth halides [41].

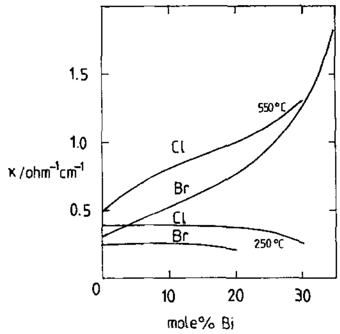

Fig. 5. Specific conductivity of mixtures of bismuth–bismuth halides [46].

alkaline earth halide systems were reported by Dworkin *et al.* [41] for some of the binary Ca, Sr and Ba halide systems. The results, shown in Fig. 4, are quite similar to the alkali systems where the Ca and Sr systems correspond to the Na systems while the Ba systems look much like the K systems. The equivalent conductivity of the dissolved metal decreases with increasing metal content in the Ca and Sr systems while the trend is opposite for the Ba systems. The authors suggested that associated species like Ca_2^{2+} are formed by dissolution of metal, Ba_2^{2+} being less stable than Sr_2^{2+} and Ca_2^{2+}. Particularly in the Ca systems, where the specific conductivity increases very little by addition of metal, localization of electrons is probable. According to Bredig [9] a little less than half the quantity of dissolved Ca in $CaCl_2$ is in the associated state in saturated mixtures. Comparison of the equivalent conductivities at infinite dilution shows that Λ_M^∞ is highest in the bromide systems. The jump distance for electrons increases with increasing size of the halide ion, and this effect, which counteracts the polarizability effect, is more significant in the alkaline earth systems than in the alkali systems due to the larger number of halide ions.

A summary of the experimental data for rare earth metal–halide systems was given by Bredig [9]. In all systems the specific conductivity of the mixture (chloride and iodide systems) increases upon addition of metal. In systems where the divalent state of the metal is stable, the electronic conductivity is low. The following equilibrium may be helpful for discussion of the experimental data

$$M^{2+} = M^{3+} + e^- \qquad (9)$$

In most of the other metal–metal halide systems which have been examined the conductivity has been measured at temperatures near the melting point of the pure salt in the salt-rich region. A summary of data was given by Bertram [42]. The majority of these systems are different from the above-mentioned systems in the sense that the specific conductivity remains nearly constant by addition of small amounts of metal. This observation indicates the formation of subvalent ions in which the excess electrons are complexed, rather than formation of mobile electrons.

Conductivity measurements reported by Grantham [43] and Suski and Stachowicz [44] show that the specific conductivity changes little by addition of Cd to the chloride, bromide and iodide. Formation of species like Cd_2^{2+}, Cd_2X_2, or atomic Cd has been proposed.

High solubilities and relatively low consolute temperatures in mixtures of bismuth and bismuth halides have led to extensive conductivity studies, e.g. by Grantham and Yosim [45], Grantham [46] and Bertram *et al.* [47]. Some results are shown in Fig. 5.

In the bromide and iodide systems the conductivity was measured for all compositions above the consolute temperatures. In the chloride and bromide systems the specific conductivity of the mixtures was found to decrease by addition of Bi near the melting point of the salts. At higher temperatures the specific conductivity increased with increasing bismuth concentration for all three systems. Above 500° C the temperature dependence of the conductivity was quite similar for the three systems. The conduction was found to be ionic up to 10 mol % Bi, semiconducting between 20 and 60 mol % Bi and metallic above 80 mol % Bi. In the semiconducting region the transport of current was assumed to take place by electron exchange between Bi^+ and Bi^{3+} ions.

Grantham [46] derived the excess conductivity from the following equation

$$\Lambda_{ex} = \Lambda_{BiX_3\text{-}Bi} - \Lambda_{BiX_3} \qquad (10)$$

where Λ_i is the product of the specific conductivity and the molar volume of the mixture. The excess molar conductivity was taken as a measure of electronic conductivity, and this contribution was found to increase strongly with increasing size of the halide ion.

In the NaF–AlF$_3$ system Borisoglebskii *et al.* [48] found that the specific conductivity increased by about 4% when Al was added to cryolite (Na_3AlF_6) at 1020° C. The excess conductivity was found to decrease when adding AlF_3 to cryolite.

A continuous transition from the metallic to the non-metallic state has been demonstrated by measurements of electrical conductivity versus composition for a few metal–molten salt systems, K–KBr, Cs–CsI, Bi–BiBr$_3$ and Bi–BiI$_3$, as shown in a review by Warren [14]. The liquid phase separation region, which appears in many systems, has prevented a more thorough investigation. There are three composition regions of interest: the metallic state, the metal–non-metal transition and the non-metallic state.

For mixtures of alkali metals and alkali halides the metal–non-metal transition is believed to be connected with localization of electrons, which leads to a sharp decrease in conductivity. Among the various mechanisms for electron localization, the F-centre model has been found to be most consistent at low metal concentrations. When the mixture contains a few mol % metal other localized states may form by disorder. Delocalization of excess electrons will occur upon further increase of the metal content. According to Warren [14], the metal–non-metal transition occurs at a lower metal concentration than the critical concentration for miscibility, typically at 5–10 mol % metal.

In the bismuth–bismuth halide systems (Fig. 5), the conductivity shows a different behaviour. The decrease in conductivity is most pronounced at 40–60 mol % metal, which suggests that the metal–non-metal transition occurs at a much higher metal concentration than for the alkali systems. In the bismuth systems, a theory for the metal–non-metal transition has been difficult to establish. This is due to the large number of different species which can be present in these mixtures.

2.4. *Electrochemical behaviour of dissolved metal*

For several molten salts there are strong indications that the metal dissolves under formation of subvalent ions. The presence of such ions makes the dissolved metal exhibit specific electrochemical properties by taking part in ionic migration or by reacting at the electrodes. Due to such reactions the electrochemical properties of dissolved metal may cause a decrease in the current efficiency during molten salt electrolysis. Experimental studies in this area have been much more scarce than investigations on metal solubility, phase diagrams and electrical conductivity. Measurements have mainly been carried out in systems where the dissolved metal is present as subvalent ions.

2.4.1. Visual observations during electrolysis. Grjotheim *et al.* [27] examined solutions of Cd in $CdCl_2$ which are characterized by intense colours. In electrolysis experiments the coloured solution was moving toward the cathode. This indicated a positive charge of the dissolved species.

As outlined in the following, Herzog and Klemm [49, 50] and Haarberg [51] observed the movement of the boundary between the coloured metal-salt solutions and the pure salt by the passage of current. In the few chloride systems investigated the dissolved metal migrated toward the cathode in some cases (Cd, Bi), toward the anode in one case (Pb) or showed no movement at all (Na, K).

Visual observations of deposition of liquid Mg in molten $MgCl_2$–NaCl showed dark clouds appearing prior to the formation of liquid metal [51]. So-called metal streamers spread from the cathode out into the melt. Haupin *et al.* [52] made visual observations of metal fog during electrolysis of $AlCl_3$ in an NaCl–KCl melt. Metal fog and bluish-grey streamers produced at the cathode disappeared when electrolysis was stopped. These phenomena were assumed to be associated with deposited Na which dissolved and subsequently reacted with $AlCl_3$, Cl_2 or H_2O.

Several observations have been reported for the industrially important system NaF–AlF_3–Al_2O_3–Al [1]. Pure molten cryolite (Na_3AlF_6) and cryolite–alumina mixtures form clear, transparent melts. By addition of aluminium to pure molten cryolite (Na_3AlF_6), fog-like streamers are produced and the melt becomes opaque. Gas bubbles and flames are often observed but this is probably a secondary phenomenon due to reaction with water impurities in the melt. It is believed that dissolved Al and Na somehow generate the fog and the colouring. Haupin and McGrew [53] made visual observations in cryolite melts and found that dark purple cathode streamers were formed when depositing Al as well as Si. They assumed that the fog contained solvated electrons (F-centres) which produced the colour. Thonstad *et al.* [54, 55] studied the formation and migration of dissolved metal in cryolite–alumina melts. The dissolved metal was found to migrate toward the anode (see Section 2.4.3).

2.4.2. Galvanic couples. Emf measurements. Emf measurements in concentration cells have been conducted only for a few binary mixtures of molten salts and metals. By varying the concentration of metal in one of the half cells, the emf data can be used to determine the chemical nature of the dissolved metal species. The factor n in the Nernst equation suggests the valence of the species. Some results, reported by Topol *et al.* [56] and by Corbett [12], are shown in Table 3.

2.4.3. Migration of dissolved metal. Subvalent ions which originate from the dissolution of metal are likely to migrate in an electric field. The fact that dissolved metals render the melts coloured while the pure molten salts usually are colourless was utilized by

Table 3. Emf studies in mixtures of molten salts and metals giving the number of electrons involved (n) *and probable dissolved species [12, 56]*

	n	*Probable dissolved species*	*Comments*
LiCl–Li	1		
KCl–NaCl–$CdCl_2$–Cd	2		
$CdCl_2$Cd	2		< 2 mol % Cd
$HgCl_2$–Hg	2		
$PbCl_2$Pb	2	Pb_2^{2+}	
PbI_2–Pb	2	Pb_2^{2+}	
SbI_3–Sb	2	SbI, Sb_2I_4	
$BiCl_3$–Bi	2	Bi^+	< 1 mol % Bi
	8	Bi_4Cl_4	7–10 mol % Bi

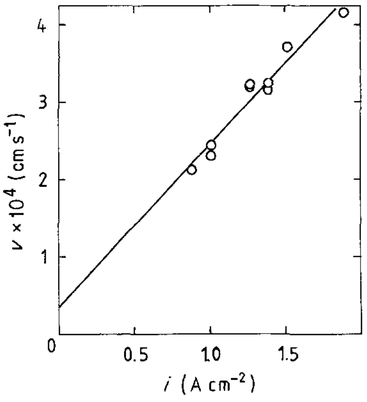

Fig. 6. The migration velocity of dissolved Cd in molten $CdCl_2$ at 610° C as a function of current density [51].

Herzog and Klemm [49, 50] to observe migration of dissolved metal in the systems $CdCl_2$–Cd and $PbCl_2$–Pb. The experimental technique was adapted from the well-known moving boundary method based on visual observations of the movement of a sharp boundary between the pure salt and the mixture of salt and metal. The results were presented as relative mobilities, i.e. the mobility of dissolved metal was referred to the movement of other ions in the electrolyte. Dissolved Cd in $CdCl_2$ migrated toward the cathode and it was found that in a saturated solution (≈ 16 mol % Cd in $CdCl_2$ at 600° C) dissolved Cd migrated 8% more slowly than Cd^{2+}, referred to the movement of Cl^-. Dissolved Pb in $PbCl_2$ was found to migrate toward the anode at a velocity 5.6 times the velocity of the Cl^- ions. At 630° C the mobility of Pb was calculated to be $34.8 \times 10^{-4}\,cm^2\,V^{-1}\,s^{-1}$ relative to the mobility of the Pb^{2+} ions. The migration velocity was found to increase with decreasing concentration of Pb. The high mobility due to dissolved Pb was discussed in terms of formation of free electrons upon dissolution of Pb.

Haarberg [51] performed migration studies in $CdCl_2$–Cd and $BiCl_3$–Bi. In both cases the boundary between the metal-containing solution and the pure molten salt was displaced toward the cathode. The mobility of dissolved Cd in $CdCl_2$ was found to be $(4.11 \pm 0.22) \times 10^{-4}\,cm^2\,V^{-1}\,s^{-1}$ at 610° C, which is 74% of the mobility of Cd^{2+} referred to the mobility of Cl^-. Figure 6 shows a plot of migration velocity versus current density. The mobility of dissolved Bi in $BiCl_3$ was $\approx 2 \times 10^{-4}\,cm^2\,V^{-1}\,s^{-1}$ at 230° C, which is twice the mobility of Bi^{3+}. These results suggested that the migrating species were Cd_2^{2+} and Bi^+. An electron exchange mechanism between Bi^+ and Bi^{3+} could account for the high mobility observed for dissolved Bi.

Thonstad and Oblakowski [55] applied a similar technique to study migration of dissolved metal in the system NaF–AlF_3–Al_2O_3–Al. The results indicated the presence of two zones of dissolved metal which moved with different velocities toward the anode. High mobilities ($\approx 20 \times 10^{-4}\,cm^2\,V^{-1}\,s^{-1}$ at 1000° C) indicated the presence of partially free electrons associated with dissolved Na.

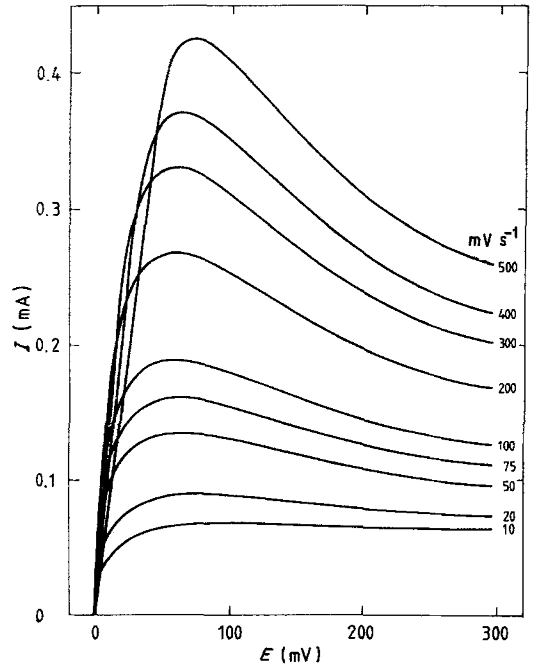

Fig. 7. Linear sweep voltammetry in molten $PbCl_2$–Pb at 566° C. Glassy carbon working electrode ($0.062\,cm^2$). Lead reference electrode [51].

2.4.4. Anodic oxidation of dissolved metal. In many cases it has been shown that dissolved metal can be oxidized at the anode in an electrochemical cell. Experimental studies in this field have mainly been conducted in binary metal–molten salt systems where the dissolved metal is present in the form of subvalent ions. These ions will oxidize to the normal valence, for example in an MX_2–M mixture

$$M_2^{2+} \longrightarrow 2M^{2+} + 2e^- \qquad (11)$$

The number of electrons transferred in the reaction and the diffusion coefficient of the subvalent ion can be determined by electrochemical techniques. Typical curves from voltammetry in $PbCl_2$–Pb are shown in Fig. 7, and chronopotentiograms obtained for anodic oxidation of Mg in $MgCl_2$ are shown in Fig. 8. Reported results are summarized in Table 4 and Fig. 9.

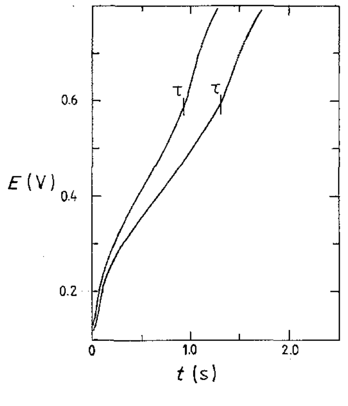

Fig. 8. Anodic chronopotentiograms in molten $MgCl_2$–Mg at 750° C. Tantalum working electrode. Mg–Pb alloy reference electrode [61].

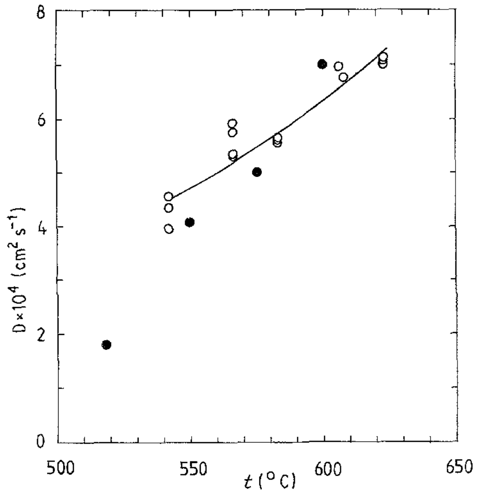

Fig. 9. Voltammetry data for the diffusion coefficient of dissolved Pb in $PbCl_2$ versus temperature. Solid line and open symbols [51]. Filled symbols [57–59].

Smirnov *et al.* [63] determined diffusion coefficients for dissolved metal in some alkali metal–alkali halide systems by using a cathodic polarization technique. The numerical values for dissolved metal at 1000° C were 1.8×10^{-4}, 5.0×10^{-4} and $1.3 \times 10^{-4}\ cm^2 s^{-1}$ in the NaCl–Na, NaBr–Na and KCl–K systems, respectively. These values are more than ten times greater than the diffusion coefficients in the pure molten salts. The authors proposed electron transitions taking place between metal atoms and cations. Also in other systems (see Table 4) the diffusion coefficient of dissolved metal is relatively high. The presence of localized electrons at low metal concentrations may lead to enhanced diffusion of the subvalent ion.

2.4.5. Polarization measurements. Wagner [64, 65] developed theories for galvanic cells with solid electrolytes exhibiting both ionic and electronic conduction. This polarization technique has been used to detect a small electronic contribution to the total conductivity. Egan and coworkers [66–70] and Huggins *et al.* [71] have applied Wagner's theories in studies of solutions of metals in molten salts.

The experimental relationship between steady state current and potential can be determined for a cell such as

$$Fe(s)\,|\,NaCl\ (1)\,|\,Na\text{–}Bi\ (1) \qquad (12)$$

by controlling either the current or the potential. The Fe electrode is made negative with respect to the Na–Bi alloy where the composition and the Na activity are known. The potential is kept below the decomposition voltage of the salt (NaCl). Due to the inertness of the Fe electrode and the high purity of the salt, ionic conduction is suppressed and the current is electronic. A concentration gradient of dissolved metal, i.e. of electrons, is established between the two electrodes.

The electronic conductivity (κ_e) can be calculated from current versus potential curves according to the equation derived by Wagner [64]

$$\kappa_e = G\frac{\partial I}{\partial E} \qquad (13)$$

where G is the cell constant. The activity of Na in the Na–Bi alloy is known from the composition and from thermodynamic data. Since the potential corresponds to a certain activity of Na at the negative (Fe) electrode, the electronic conductivity can be determined as a function of the activity of Na in the salt. Results obtained by using the polarization method in NaCl–Na, as reported by Egan *et al.* [70], are shown in Figs 10 and 11.

The diffusion coefficient of electrons in mixtures of molten alkali halides and alkali metals was determined by applying a transient technique in cells similar to (12) [69, 70]. The mobility of electrons, which was calculated from the Nernst–Einstein equation, was found to be constant in the metal activity range of ~0.001–0.1. Table 5 gives a summary of results obtained by using the Wagner polarization technique.

2.5. *Other properties*

A large number of experimental studies concerning other properties of mixtures of metal and molten salts have been reported. Literature references can be found in a review written by Warren [13].

Table 4. Anodic oxidation of dissolved metal in molten salts; reactions, diffusion coefficients (D) *and techniques used*

	Reaction	*T (° C)*	*$10^5 \times D\ (cm^2 s^{-1})$*	*Technique*	*References*
$PbCl_2$–Pb	$Pb_2^{2+} \longrightarrow 2Pb^{2+} + 2e^-$	518	1.8	Chronopotentiometry, voltammetry	[57, 58]
	$Pb_2^{2+} \longrightarrow 2Pb^{2+} + 2e^-$	550	4.1	Chronopotentiometry	[59]
		575	5.0		
		600	7.0		
	$Pb_2^{2+} \longrightarrow 2Pb^{2+} + 2e^-$	566	5.6 ± 0.3	Linear sweep voltammetry	[51]
$ZnCl_2$–Zn	$Zn_2^{2+} \longrightarrow 2Zn^{2+} + 2e^-$	500	0.8	Chronopotentiometry	[58, 59]
		525	2.3		
		600	2.8		
$BiCl_3$–Bi	$Bi^+ \longrightarrow Bi^{3+} + 2e^-$	420	1.2	A.c. impedance	[60]
$MgCl_2$–Mg	$Mg_2^{2+} \longrightarrow 2Mg^{2+} + 2e^-$	750	0.5	Chronopotentiometry	[61]
AgCl–Ag	$Ag_n^{(n-1)+} \longrightarrow nAg^+ + e^-$	520	2.0	Chronopotentiometry	[62]
AgBr–Ag	$Ag_n^{(n-1)+} \longrightarrow nAg^+ + e^-$	500	4.2	Chronopotentiometry	[62]
Na_3AlF_6–Al_2O_3–Al	$AlF_2^- + F^- \longrightarrow AlF_3 + 2e^-$	1000	10.9 ± 2.6	Linear sweep voltammetry	[33]
		1000	10.1 ± 2.1	Chronopotentiometry	[33]

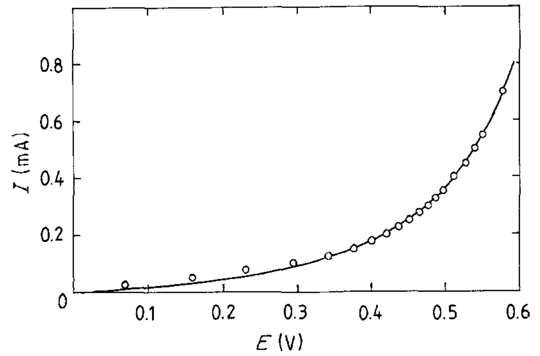

Fig. 10. Current versus potential from polarization experiment in molten NaCl–Na at 900° C. Experimental data and fitted curve [69].

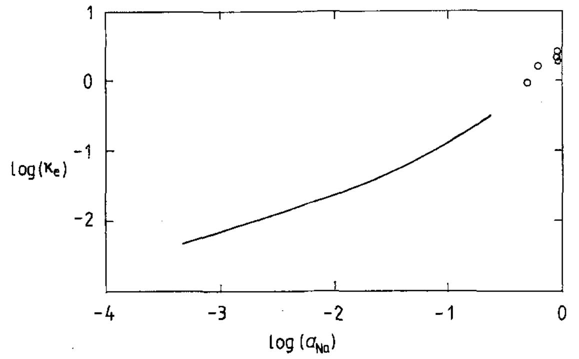

Fig. 11. Electronic conductivity as a function of Na activity in molten NaCl at 850° C. Solid line: Calculated from polarization experiment [69].

Thermodynamic properties such as Gibbs energy, enthalpy and activity of dissolved metal have been determined from calorimetric studies, cryoscopy and measurements of vapour pressure and emf. Density and viscosity have also been determined for some mixtures. The use of magnetic measurements has increased in recent years. Studies of magnetic susceptibility, nuclear magnetic resonance and electron spin resonance have proved to be particularly useful for assessing electronic properties and the metal–non-metal transition. Optical properties have also been studied.

2.6. *Related systems*

Some other systems show similarities to mixtures of molten salts and metals in certain respects. Particularly, this concerns visual appearance and electrical properties in solid electrolytes, solid ionic crystals with excess electrons and mixtures of liquid ammonia and metals. Studies of such systems may contribute to a better understanding of the properties and the nature of dissolved metal in molten salts.

2.6.1. Excess metal in solid crystals. Solid electrolytes may show ionic conduction due to lattice defects. Incorporation of metal may give rise to migration of electrons, and the electronic conductivity can be determined. Such studies were reported by Wagner [72] for AgBr–Ag and by Wagner and Wagner [73] for cuprous halides in contact with Cu. Delcet *et al.* [74] studied electronic conductivity in solid CaF_2 in equilibrium with Ca alloys at 800–950° C. The ionic transport number was found to decrease from 0.98 to 0.68 when the calcium activity increased from 10^{-3} to unity.

Solid crystals of pure salts are usually transparent and often colourless. Colouration of crystals may take place by irradiation (electrons, neutrons) or by addition of excess metal or by electrolysis. Some of the properties of coloured crystals are related to the presence of electrons in the conduction band. Electrons can be localized at anion sites in the lattice, and this configuration is designated F-centre (colour centre). According to Ukshe and Bukun [11] the intensity of the colour increases with increasing temperature, and the electronic conductivity of doped crystals increases exponentially with temperature.

Stasiw [75] studied the movement of colour centres in alkali halide crystals. A sharp blue colour was produced at the cathode during electrolysis, and the movement of the coloured zone toward the anode was observed visually. The mobility of colour centres in KCl crystals was determined to be $\cong 5.2 \times 10^{-4}$ cm^2 V^{-1} s^{-1} at 650° C. In sodium and potassium halides the mobility increased with increasing temperature and increasing size of the anion. Similar experiments were conducted by Smakula [76]. Heiland [77] studied the colouring of crystals of KCl and KI by electrolysis. In KI a brown colour which was produced at the anode migrated toward the cathode whereas a blue colour which appeared at the cathode moved in the

Table 5. Electronic conductivity and diffusion coefficient of electrons from polarization measurements

Molten salt	*Reference electrode*	*Temperature t (° C)*	*Metal activity*	*Electronic conductivity κ_e (ohm^{-1} cm^{-1})*	*Diffusion coefficient D (cm^2 s^{-1})*	*References*
LiCl-KCl	Li-Al	383	5.6×10^{-2}	8×10^{-5}		[71]
		383	1	0.01		
		465	0.01	4×10^{-3}		
		465	1	0.18		
NaCl	Na-Bi	850	0.14	0.216	0.0093	[69]
		850	0.23	0.366	0.0095	
		900	0.14	0.354	0.0120	
		900	0.23	0.483	0.0123	
NaBr	Na-Bi	850	0.17	0.992	0.210	[70]
NaI	Na-Bi	850	0.18	0.930	0.170	[70]

opposite direction. The two clouds can be attributed to trapped holes and trapped electrons, respectively. Similar colour changes were observed by Haarberg [51] during electrolysis of pure molten salts.

2.6.2. Dissolved metal in liquid ammonia. Solutions of alkali metals and alkaline earth metals in liquid NH_3 have much in common with solutions of the same metals in molten salts. Physicochemical and electrical properties have been examined and models have been suggested to explain the observations made. The shape of the phase diagrams are similar to those of the metal–metal halides. The miscibility gap is, however, narrower and it is displaced to much lower metal contents. Edwards [78] has summarized the electronic properties of solutions of metal in NH_3 and organic solvents as well. Small quantities of sodium dissolved in NH_3 have been found to make the mixture turn intensely blue, and localized electrons, sodium cations and various agglomerates of these were assumed to be present. According to Mott [79] dilute solutions of Na in NH_3 are completely dissociated with electrons localized in cavities. The specific conductivity of these mixtures increases strongly with increasing concentration of dissolved metal. The transition from nonmetal to metal was detected at 2.4 mol % Na, as reported by Pitzer [21]. According to Mott [79] the metal concentration corresponding to this transition decreases with increasing temperature. In some of the binary systems solid phases have been observed, e.g. $Li(NH_3)_4$ and $Ca(NH_3)_6$ [80]. A comprehensive treatment of solutions of metals in liquid ammonia was given by Thompson [81].

3. Structure and nature of dissolved metal. Theoretical models

Existing models have mainly been based on electronic properties of mixtures of metals and molten salts. The attention has been focused on experimental data for electrical conductivity and magnetic properties, particularly for mixtures of alkali metals and alkali halides. The following models have been proposed: free electron model (dilute free electron gas); localization (trapped electron or localization due to random disorder); band models.

Symons [80] discussed solutions of metals in various systems. The presence of localized electron centres have been established in solid alkali halide crystals doped with metal: F-centre – an electron trapped in an anion vacancy; F′-centre – two electrons trapped in the same anion vacancy; M-centre – two electrons occupying two adjacent anion vacancies (i.e. two adjacent F-centres).

Electron spin resonance spectroscopy reported by Symons [80] shows that F-centres are the most stable. F′-centres and M-centres may be formed at higher concentrations of trapped electrons.

Also for metal–molten salt systems models based on the formation of trapped electrons seem to give a good description of the observed behaviour, and such models are favoured by most authors. For high concentrations of metal the picture is less clear, but the presence of free electrons has been proposed by several authors. However this concentration range is not considered in the present treatment.

For the dilute range some authors have proposed models which differ from the trapped electron concept, and some of these will be briefly mentioned. Rice [82] suggested that the excess electrical conductivity of dissolved metal in its own salt is due to random walk of the electrons between atoms and metal ions, e.g. a thermally activated hopping model. The calculated electron mobility was in agreement with the experimental data. Katz and Rice [83] suggested the presence of: (1) localized states with trapped electrons at low metal concentration; (2) nearly free electrons scattered by the anions in mixtures with more than 50 mol % metal.

In the sodium systems the electrons due to dissolved Na were assumed to be in the extended states at low metal concentration of dissolved metal and above a certain concentration ($\cong$10 mol % Na in NaBr) the mobility of Na starts to increase. Electrons occupying localized states were claimed to exhibit a thermally activated mobility with a positive temperature coefficient.

Durham and Greenwood [84] proposed that dissolved metal dissociated into metal cations and electrons, and nearly-free electrons in the conduction band scattered by the ions of the melt could be responsible for the observed electronic conductivity of the potassium and sodium systems. The proportion of conducting electrons of the excess metal was calculated to be 0.13 for NaCl with 0–5 mol % Na at 845° C. For KBr–K at 760° C this proportion increased from 0.17 at 1 mol % to 0.27 at 5 mol % K. Since Na is more electronegative than K and has a higher ionization potential, Na is more likely to attach an electron.

Emi and Bockris [85] calculated the mobility of electrons in NaCl–Na and KCl–K at low metal concentrations by assuming that the electrons are transferred from the metal atom to a neighbouring ion by hopping followed by tunnelling. Electrons were assumed to be well localized in the salt-rich region. Delocalization was likely to occur at higher metal concentrations, particularly for KCl–K. The calculated mobilities were in agreement with literature data. However, the concentration dependence was not confirmed because interactions between metal atoms were neglected.

Nachtrieb [86] summarized three previously proposed models: free electrons; thermally activated hopping; F-centres. Among these the F-centre model, which was proposed by Pitzer [21] (see Section 2.2.1), was believed to be the most promising in explaining the properties of mixtures of alkali metals and molten alkali halides in the salt-rich region. An F-centre may be regarded as a localized state, according to Nachtrieb [86], and the electron is then trapped in a cavity with octahedral coordination with the neighbouring cations. On average the centre may be considered as an M_6^{5+}

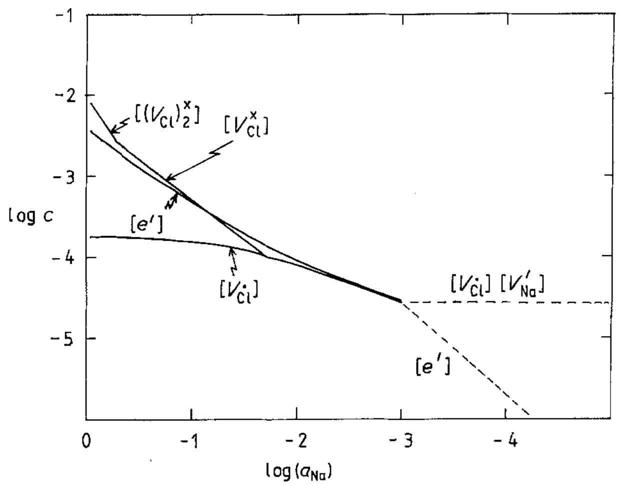

Fig. 12. The defect concentration [moles of defects/moles of NaCl] as a function of Na activity in molten NaCl at 850° C [69]. e′-electron, V′-cation vacancy, V′-anion vacancy, V_{Cl}^x – F-centre, $(V_{Cl})_2^x$ – F-centre dimer.

species. The F-centre model was supported by Warren *et al.* [39] based on nuclear magnetic resonance measurements. The constant electronic mobility in NaBr–Na at low metal concentration was attributed to the formation of non-magnetic and non-conducting species.

Also Nicoloso and Freyland [87] and Freyland and Nattland [40] interpreted their results from electron spin resonance studies and electrical conductivity measurements in alkali metal–alkali halides in terms of formation of F-centres at low metal concentration. Equilibrium between F-centres and diamagnetic species such as metal dimers (M_2) or metal anions (M^-) was considered. At increasing metal concentration association to F-centre dimers and trimers was proposed.

Egan and Freyland [88] developed a thermodynamic model for salt-rich NaBr–Na mixtures, which was later extended to other alkali halide–alkali metal systems [70]. It was based on studies of solid alkali halides with excess metal by Kroger [89] and Wagner [90]. In the pure stoichiometric molten salt the concentrations of electrons and electron holes were assumed to be equal. On addition of metal the following defects were considered: electrons, F-centres and F-centre dimers. A number of chemical equilibria involving these defects was proposed, and by applying the law of mass action quantitative relationships could be obtained. Figure 12 shows the concentration of defects as a function of the activity of Na in NaCl at 850° C. Thermodynamic data of Smirnov *et al.* [63] were used in the calculations. The defect model has also successfully been fitted to data from spectroscopic, magnetic and conductivity measurements. Hence the model provides a quantitative correlation between thermodynamics and other physical properties of the systems.

References

[1] K. Grjotheim, C. Krohn, M. Malinovsky, K. Matiasovsky and J. Thonstad, 'Aluminium Electrolysis', Aluminium-Verlag, Dusseldorf (1982).

[2] K. Andreassen, *Erzmetall.* **31** (1978) 301.

[3] W. Kunz and P. Klencz, in Ullmann: 'Encyclopedia der technischen Chemie', 4th edn Chemie, Weinheim (1979) Vol. 17, p. 143.

[4] E. Coley, in 'Molten Salt Technology' (edited by D. G. Lovering), Plenum Press, New York (1982) p. 57.

[5] A. H. W. Aten, *Z. Phys. Chem.* **66** (1909) 641.

[6] A. H. W. Aten, *Z. Phys. Chem.* **73** (1910) 578.

[7] R. Lorenz, G. V. Hevesy and E. Wolff, *Z. Phys. Chem.* **76** (1911) 732.

[8] M. A. Bredig, J. W. Johnson and W. T. Smith Jr, *J. Am. Chem. Soc.* **77** (1955) 307.

[9] M. A. Bredig, in 'Molten Salt Chemistry' (edited by M. Blander), Interscience, New York (1964) p. 367.

[10] D. Cubicciotti, *J. Metals* **5** (1953) 1106.

[11] E. A. Ukshe and N. G. Bukun, *Russ. Chem. Rev.* **30** (1961) 90.

[12] J. D. Corbett, in 'Fused Salts' (edited by B. R. Sundheim), McGraw-Hill, New York (1964) p. 341.

[13] W. W. Warren Jr, in 'Advances in Molten Salt Chemistry' (edited by G. Mamantov and J. Braunstein), Plenum Press, New York (1981) Vol. 4, p. 1.

[14] W. W. Warren Jr, in 'The Metallic and Nonmetallic States of Matter' (edited by P. P. Edwards and C. N. R. Rao), Taylor and Francis, London (1985) p. 39.

[15] J. D. Corbett and S. von Winbush, *J. Am. Chem. Soc.* **77** (1955) 3964.

[16] J. D. Corbett, S. von Winbush and F. C. Albers, *J. Am. Chem. Soc.* **79** (1957) 3020.

[17] J. D. Corbett, W. J. Burkhard and L. F. Druding, *J. Am. Chem. Soc.* **83** (1961) 76.

[18] E. M. Levin, C. R. Robbins and H. F. McMurdie (editors), 'Phase Diagrams for Ceramists', The American Ceramic Society (1964, 1967, 1975).

[19] A. S. Dworkin, H. R. Bronstein and M. A. Bredig, *J. Phys. Chem.* **66** (1962) 572.

[20] M. A. Bredig and H. R. Bronstein, *J. Phys. Chem.* **64** (1960) 64.

[21] K. S. Pitzer, *J. Am. Chem. Soc.* **84** (1962) 2025.

[22] S. J. Yosim, D. J. Darnell, W. G. Gehman and S. W. Mayer, *J. Phys. Chem.* **63** (1959) 230.

[23] S. J. Yosim, L. D. Ransom, R. W. Sallach and L. E. Topol, *J. Phys. Chem.* **66** (1962) 28.

[24] A. Hershaft and J. D. Corbett, *Inorg. Chem.* **2** (1963) 979.

[25] J. D. Corbett and R. E. Rundle, *Inorg. Chem.* **3** (1964) 1408.

[26] L. E. Topol and A. L. Landis, *J. Am. Chem. Soc.* **82** (1960) 6291.

[27] K. Grjotheim, F. Grønvold and J. Krogh-Moe, *J. Am. Chem. Soc.* **77** (1955) 5824.

[28] D. Cubicciotti, *J. Am. Chem. Soc.* **74** (1952) 1198.

[29] J. Thonstad, *Can. J. Chem.* **42** (1964) 2739.

[30] J. Thonstad, *Can. J. Chem.* **43** (1965) 3429.

[31] M. M. Vetyukov and V. B. Vinkokurov, 'Physical Chemistry and Electrochemistry of Molten Salts and Slags', Naukova Dumka, Kiev (1969) p. 367.

[32] R. Ødegård, Å. Sterten and J. Thonstad, *Met. Trans.* **19B** (1988) 444.

[33] K. Yoshida, T. Ishihara and M. Yokoi, *Trans. Met. Soc. AIME* **242** (1986) 231.

[34] J. P. Saget, V. Plichon and J. Badoz-Lambling, *Electrochim. Acta* **20** (1975) 825.

[35] V. N. Storozhenko, *Russ. J. Phys. Chem.* **46** (1972) 1227.

[36] V. Ya. Kudyakov and M. V. Smirnov, *J. Appl. Chem. USSR* **53** (1980) 741.

[37] H. R. Bronstein and M. A. Bredig, *J. Am. Chem. Soc.* **80** 2077 (1958).

[38] H. R. Bronstein and M. A. Bredig, *J. Phys. Chem.* **65** (1961) 1220.

[39] W. W. Warren Jr, S. Sotier and G. F. Brennert, *Phys. Rev. Lett.* **50** (1983).

[40] W. Freyland and D. Nattland, private communication, University of Karlsruhe.

[41] A. S. Dworkin, H. R. Bronstein and M. A. Bredig, *J. Phys. Chem.* **70** (1966) 189.

[42] R. Bertram, *Z. Anal. Chem.* **222** (1966) 189.

[43] L. F. Grantham, *J. Chem. Phys.* **44** (1966) 1509.

[44] L. Suski and L. Stachowicz, *Electrochim. Acta* **17** (1972) 1987.

[45] L. F. Grantham and S. J. Yosim, *J. Chem. Phys.* **38** (1963) 1671.

[46] L. F. Grantham, *J. Chem. Phys.* **43** (1965) 1415.

[47] R. Bertram, P. Lambrecht and D. Wiebe, *Metalloberflache* **24** (1970) 120.

[48] Yu. Borisoglebskii, M. M. Yetyukov and S. Abi-Zeid, *Tsvetn. Met.* **51** (1978) 41.

[49] W. Herzog and A. Klemm, *Z. Naturforschung* **15a** (1960) 1100.

[50] W. Herzog and A. Klemm, *Z. Naturforschung* **16a** (1961) 5239.

[51] G. M. Haarberg, 'Electrochemical Properties of Dissolved Metal in Molten Salts', Doctorate thesis, The University of Trondheim, NTH (1985).

[52] W. E. Haupin, R. S. Danchik and J. W. Luffy, 'Light Metals', The Metallurgical Society of AIME, Warrendale, PA, USA (1976) Vol. 1, p. 159.

[53] W. E. Haupin and W. C. McGrew, *Aluminium* **51** (1975) 273.

[54] J. Thonstad and S. Rolseth, 'Light Metals', The Metallurgical Society of AIME, Warrendale, PA, USA (1976) Vol. 1, p. 171.

[55] J. Thonstad and R. Oblakowski, *Electrochim. Acta* **25** (1980) 223.

[56] L. E. Topol, S. J. Yosim and R. A. Osteryoung, *J. Phys. Chem.* **65** (1961) 1511.

[57] J. J. Egan, *J. Phys. Chem.* **65C** (1961) 2222.

[58] J. D. Van Norman, J. S. Bookless and J. J. Egan, *J. Phys. Chem.* **70** (1966) 1276.

[59] M. M. Yetyukov and A. Fransis, *Sov. Electrochem.* **5** (1969) 331.

[60] T. A. Lavrova and R. Yu. Bek, *Sov. Electrochem.* **5** (1969) 52.

[61] J. D. van Norman and J. J. Egan, *J. Phys. Chem.* **67** (1963) 2460.

[62] J. D. van Norman, *J. Electrochem. Soc.* **112** (1965) 1126.

[63] M. V. Smirnov, V. V. Chebykin and L. A. Tsiovkina, *Electrochim. Acta* **26** (1981) 1275.

[64] C. Wagner, *Proc. CITCE* **7** (1957) 361.

[65] J. B. Wagner and C. Wagner, *J. Chem. Phys.* **26** (1957) 1597.

[66] R. J. Heus and J. J. Egan, *J. Phys. Chem.* **77** (1973) 1989.

[67] R. J. Heus and J. J. Egan, 'Proc. Int. Symp. Molten Salts', Electrochem. Soc., Princeton (1976) p. 523.

[68] R. E. Davis, R. J. Heus and J. J. Egan, 'Proc. Second Int. Symp. Molten Salts', Electrochem. Soc., Princeton (1981).

[69] G. M. Haarberg, K. S. Osen and J. J. Egan, 'Proc. Joint Int. Symp. Molten Salts' (1987) p. 235.

[70] G. M. Haarberg, K. S. Osen, J. J. Egan, H. Heyer and W. Freyland, *Ber. Bunsenges. Phys. Chem.* **92** (1988) 139.

[71] G. J. Reynolds, M. C. Y. Lee and R. A. Huggins, 'Proc. Fourth Int. Symp. Molten Salts', Electrochem. Soc., Princeton (1983) p. 519.

[72] C. Wagner, *Z. Electrochem.* **60** (1956) 4.

[73] J. B. Wagner and C. Wagner, *J. Chem. Phys.* **26** (1957) 1597.

[74] J. Delcet, R. J. Heus and J. J. Egan, *J. Electrochem. Soc.* **125** (1978) 755.

[75] O. Stasiw, *Nachr. Ges. Wiss. Gottingen II* **50** (1933) 387.

[76] A. Smakula, *Nachr. Ges. Wiss. Gottingen, Math-Physik Kl.II* **1** (4) (195).

[77] G. Heiland, *Z. Phys.* **127** (1950) 144.

[78] P. P. Edwards, *Phys. Chem. Liq.* **10** (1981) 198.

[79] N. F. Mott, *Adv. Phys.* **16** (1967) 49.

[80] M. C. R. Symons, *Chem. Soc. Rev.* **5** (1976) 337.

[81] J. C. Thompson, 'Electrons in Liquid Ammonia', Clarendon Press, Oxford (1976).

[82] S. A. Rice, *Discuss. Faraday Soc.* **32** (1961) 181.

[83] I. Katz and S. A. Rice, *J. Am. Chem. Soc.* **94** (1972) 4824.

[84] P. J. Durham and D. A. Greenwood, *Phil. Mag.* **33** (1976) 427.

[85] T. Emi and J. O'M. Bockris, *Electrochim. Acta* **16** (1971) 2081.

[86] N. H. Nachtrieb, *Adv. Chem. Phys.* **31** (1975) 465.

[87] N. Nicoloso and W. Freyland, *J. Phys. Chem.* **87** (1983) 1997.

[88] J. J. Egan and W. Freyland, *Ber. Bunsenges. Phys. Chem.* **89** (1985) 381.

[89] F. A. Kroger, 'The Chemistry of Imperfect Crystals', Vol. 2, 2nd edn, North Holland, American Elsevier (1974).

[90] C. Wagner, *Ber. Bunsenges. Phys. Chem.* **77** (1973) 518.